Chemical Science

EDGE ARTICLE

View Article Online
View Journal | View Issue

Cite this: *Chem. Sci.*, 2015, **6**, 3236

Very bright mechanoluminescence and remarkable mechanochromism using a tetraphenylethene derivative with aggregation-induced emission†

Bingjia Xu,‡[ab] Jiajun He,‡[a] Yingxiao Mu,[a] Qiangzhong Zhu,[b] Sikai Wu,[a] Yifan Wang,[c] Yi Zhang,*[a] Chongjun Jin,[b] Changcheng Lo,[c] Zhenguo Chi,*[a] Alan Lien,[d] Siwei Liu[a] and Jiarui Xu*[a]

Received 7th February 2015
Accepted 16th March 2015

DOI: 10.1039/c5sc00466g

www.rsc.org/chemicalscience

Organic materials exhibiting mechanoluminescence (ML) are promising for usage in displays, lighting and sensing. However, the mechanism for ML generation remains unclear, and the light-emitting performance of organic ML materials in the solid state has been severely limited by an aggregation-caused quenching (ACQ) effect. Herein, we present two strongly photoluminescent polymorphs (*i.e.*, C_g and C_b) with distinctly different ML activities based on a tetraphenylethene derivative P_4TA. As an aggregation-induced emission (AIE) emitter, P_4TA perfectly surmounted the ACQ, making the resultant block-like crystals in the C_g phase exhibit brilliant green ML under daylight at room temperature. The ML-inactive prism-like crystals C_b can also have their ML turned on by transitioning toward C_g with the aid of dichloromethane vapor. Moreover, the C_g polymorph shows ML and mechanochromism simultaneously and respectively without and with UV irradiation under a force stimulus, thus suggesting a feasible design direction for the development of efficient and multifunctional ML materials.

Introduction

The mechanoluminescence (ML) phenomenon was first found by Francis Bacon in 1605.[1] Heretofore, research on exploiting advanced ML materials has not yet been a major focus.[2] Materials with brilliant ML are actually of great importance from both fundamental and practical viewpoints because they are promising for usage in displays, as well as light sources and sensors.[2,3] However, a comprehensive understanding of the crystal properties required for ML activity and the corresponding mechanisms is less well demonstrated.[4] This lack in understanding leads to feasible design principles for these emitters, particularly those with satisfactory ML brightness, being rarely found.[5] As reported previously, the performance of organic ML compounds can be related to both their molecular and molecular-assembly structures.[6] Therefore, controlling the molecular arrangements in the solid state and achieving a molecular-level understanding of the relationship between the molecular conformations and packing characteristics and the resulting optical properties are the essential issues in obtaining efficient ML materials.

Notably, non-covalent intermolecular interactions, such as π–π stacking and hydrogen bonding, are important in constructing the supramolecular systems.[7] These interactions are able to influence the final packing structure strongly, thereby making polymorphism with different ML activities more probable.[6a,8] Nevertheless, in most cases, typical π–π stacking interactions often lead to aggregation-caused quenching, which poses significant difficulties for development of high-performance ML materials.[4b,9] By contrast, a diametrically opposed effect was recently found to be operative in a class of chromophores with twisted conformations (*e.g.*, tetraphenylethene derivatives), which exhibit enhanced emission in the solid state with respect to the fluid solution.[10] The discovery of this abnormal phenomenon, known as aggregation-induced emission (AIE), has sparked a rapid expansion in the field of photoluminescent sensors and electroluminescent devices.[11] AIE also provides new possibilities for designing highly mechanoluminescent materials.

This study presents a new polymorphic system that can be facilely and controllably constructed using a tetraphenylethene

[a]*PCFM Lab, GD HPPC Lab, Guangdong Engineering Technology Research Center for High-performance Organic and Polymer Photoelectric Functional Films, State Key Laboratory of Opto-electronic Material and Technologies, School of Chemistry and Chemical Engineering, Sun Yet-sen University, Guangzhou 510275, China. E-mail: ceszy@mail.sysu.edu.cn; chizhg@mail.sysu.edu.cn; xjr@mail.sysu.edu.cn; Fax: +86 20 84112222; Tel: +86 20 84112712*

[b]*State Key Laboratory of Optoelectronic Material and Technologies, School of Physics and Engineering, Sun Yat-sen University, Guangzhou 510275, China*

[c]*Shenzhen China Star Optoelectronics Technology Co., Ltd, Guangdong, China*

[d]*TCL Corporate Research, Guangdong, China*

† Electronic supplementary information (ESI) available: Details of the synthesis; structural information for the compound (NMR, IR, and mass spectra); Tables S1–S5; Fig. S1–S11. CCDC 1037840 and 1057432. For ESI and crystallographic data in CIF or other electronic format see DOI: 10.1039/c5sc00466g

‡ These authors contributed equally to the preparation of this work.

derivative [*i.e.*, 5-(4-(1,2,2-triphenylvinyl)phenyl)thiophene-2-carbaldehyde (P_4TA)] as the building block (Fig. 1). The two crystalline polymorphs of P_4TA show strong blue- and green-colored photoluminescence (PL). The blue-light crystals are significantly ML inactive, whereas the green-light ones are highly mechanoluminescent because of their distinctly different molecular packing mode and unique AIE character. The existence of polymorphs from the same molecule with exactly opposite properties provides a unique prototype to investigate the crystalline structures required for ML activity and the effect of AIE properties on ML enhancement. The relationship between the ML and the mechanofluorochromism of P_4TA is also presented.

Results and discussion

P_4TA was straightforwardly prepared through a palladium-catalyzed coupling reaction by introducing 2-thiophenaldehyde to the tetraphenylethene moiety (Scheme S1†). The purified material was then characterized using nuclear magnetic resonance (NMR) spectroscopy and X-ray crystallography. The satisfactory data obtained fully confirmed its expected molecular structure (ESI†).

The UV-visible absorption spectrum of P_4TA was measured in a dichloromethane (DCM) solution. Two absorption bands centered at 317 and 366 nm were observed. These two bands were associated with the π–π* transition and intramolecular charge transfer, respectively (Fig. S1†). The large Stokes shift (68 027 cm^{-1}) between the absorption and fluorescence spectra ($\lambda_{em,max}$ = 513 nm) of P_4TA in DCM was indicative of the structural difference between the ground and excited states. The resulting P_4TA compound would probably also be AIE-active on considering that tetraphenylethene is the most frequently used AIE unit. To confirm this probability, a tetrahydrofuran (THF) solution of P_4TA was titrated with water and the change in the fluorescence emission was monitored. P_4TA exhibited an extremely weak emission in the THF solution, where it was well dissolved (Fig. 2a). Hence, almost no PL signal was recorded. However, when 90% (v/v) water was present, a strong green emission that peaked at 499 nm was observed and the corresponding intensity (~705 a. u.) dramatically increased by up to ~100 times compared to that at the 0% water fraction (~7 a. u.). Adding water to the THF solution of P_4TA significantly induced the formation of nanoparticles because P_4TA molecules contain highly hydrophobic aromatic rings. In other words, the emission enhancement was caused by molecule aggregation which suggests that P_4TA is AIE-active.[12]

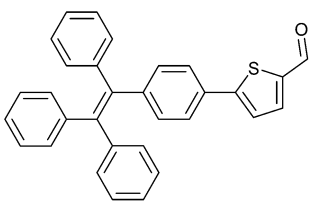

Fig. 1 Molecular structure of P_4TA.

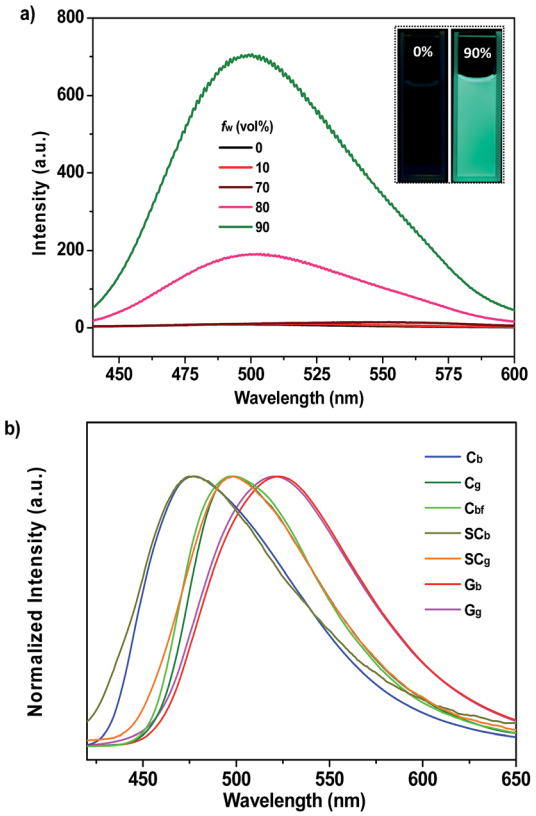

Fig. 2 (a) PL spectra of dilute solutions of P_4TA in water–THF mixtures with different water fractions (f_w). The inset depicts the emission images of the compound in pure THF and in the 90% water fraction mixture under 365 nm UV illumination (10 μM). (b) PL spectra of P_4TA in different phases.

The prominent AIE character of P_4TA motivated the application of the material in the solid state. Accordingly, block-like crystals (C_g-form) were achieved through solvent evaporation of P_4TA in a mixed solvent of *n*-hexane and DCM (Fig. S2a†). Compared to the emissive nanoaggregates in THF–H_2O, the as-prepared sample C_g exhibited an even stronger green-light emission, centered at 498 nm [$\Phi_{F,s}$ = 52%] (Fig. 2b). By grinding the C_g crystals with a pestle or shearing them with a spatula, a very bright green light emission peaking at 517 nm was observed in the dark without UV irradiation (Fig. 3a and c and Video S1†). This experiment unambiguously illustrated that P_4TA in the C_g-form was ML-active. The strong ML of C_g was indeed clearly seen even under daylight at room temperature and was maintained while the crystals were crushed (Fig. 3c and Video S2†). Certain organic materials, such as coumarin, phenanthrene, *N*-acetyl anthranilic acid, *N*-isopropyl carbazole and *N*-phenyl imides, have also been reported to show mechanoluminescence activities. However, none of these materials could emit a ML strong enough to be observed with the naked eye under daylight at room temperature.[5,13] The poor performance of the conventional organic ML materials should be attributed to their intrinsic ACQ property, which leads to the low emitting efficiency in the solid state. By contrast, the unique AIE feature of P_4TA perfectly surmounted the ACQ effect and

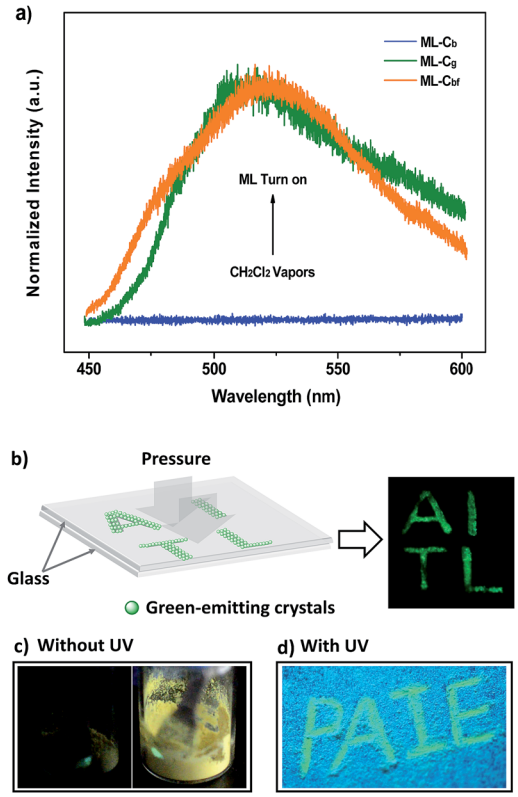

Fig. 3 (a) ML spectra of P_4TA in different phases. (b) An image of the capital letters 'AITL' being shown through ML of P_4TA in the dark under a pressure stimulus at room temperature. (c) ML images of P_4TA in the dark (left) and under daylight (right) at room temperature. (d) The writable mechanochromic fluorescence of P_4TA, demonstrated using the capital letters 'PAIE', generated with a metal rod.

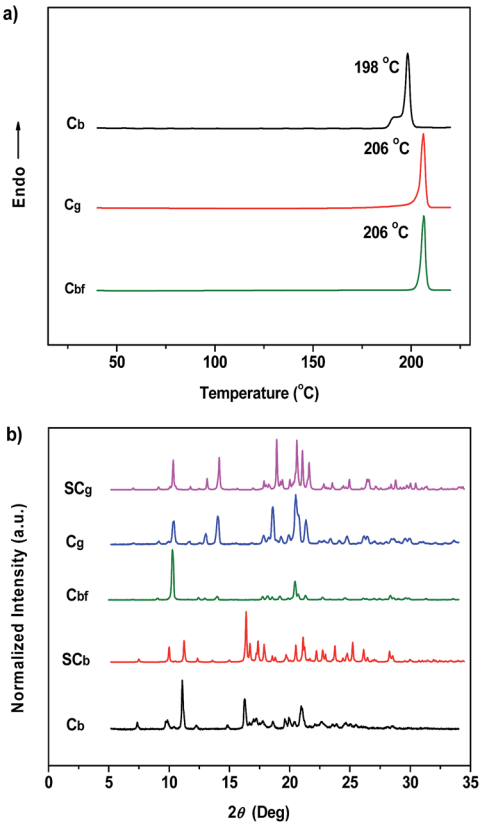

Fig. 4 DSC curves (a) and XRD patterns (b) of P_4TA in different phases.

exhibited a positive effect on luminescence enhancement, thereby giving the brilliant ML of C_g. To further demonstrate the ML characteristics of C_g, a simple device was made by sandwiching the sample between two pieces of pre-sculptured glass. The capital letters 'AITL' were clearly displayed when pressure was used as the driving force, which suggests the ML 'display capability' of C_g (Fig. 3b). As such, the extraordinary AIE-active ML material P_4TA will be a promising candidate for displays and optical recording.

Interestingly, another type of prism-like crystal (C_b-form) was observed while exploring different processing conditions. The C_b-form crystals, which showed an intense blue-light emission that peaked at 476 nm ($\Phi_{F,s}$ = 36%), could be obtained by adding ethanol into a P_4TA/DCM solution under the action of ultrasound (Fig. S2b†). However, in contrast to the vivid C_g phenomenon, the P_4TA sample completely lost its ML activity when aggregated in the C_b-form (Fig. 3a). The C_b crystals showed a small melting endothermic shoulder peak at 191 °C and a sharp peak at 198 °C in the first heating curve of differential scanning calorimetry (DSC) (Fig. 4a), indicating that C_b was mainly composed of microcrystals that melt at 198 °C. This result is different from that of C_g, which melts at 206 °C. Moreover, the powder X-ray diffraction (XRD) spectra also exhibited distinctly different patterns for the two samples (Fig. 4b). These results imply that the different ML activities of C_g and C_b could be attributed to their dissimilar molecular packing modes. A single crystal X-ray analysis was thus performed for the P_4TA crystals to obtain more insight into this aspect. Single crystals of the two polymorphs (*i.e.*, SC_g and SC_b) suitable for X-ray structural analysis were isolated through slow solvent evaporation of P_4TA in mixtures of ethanol and $CHCl_3$ of different concentrations.

The SC_g and SC_b samples emitted intense green or blue light peaked at 499 and 476 nm, respectively (Fig. 2b and 5a and b). These light emissions are similar to those of the as-prepared crystals of C_g and C_b. The main peaks of the simulated XRD patterns of SC_g and SC_b also agree well with those in the patterns obtained from P_4TA in the C_g and C_b phases, which suggests that the initial powders were mainly composed of P_4TA microcrystals in the polymorphs of SC_g and SC_b (Fig. 4b). Further systematic analysis revealed that both SC_g and SC_b belong to the non-centrosymmetric polar space group of $P(2)1$ (Table S1†). Some previous reports have shown that dipolar structures and non-centrosymmetric molecular arrangements are favorable for obtaining piezoelectric properties, which were closely pertinent to the ML activities of the crystals.[14] In principle, the fracture of crystals with a strong piezoelectric effect will lead to electronic discharge at the crack surface, which would result in dye excitation and generation of ML for the crystals.[5,15] The molecular structure of P_4TA and the crystalline symmetry of SC_g and SC_b also meet

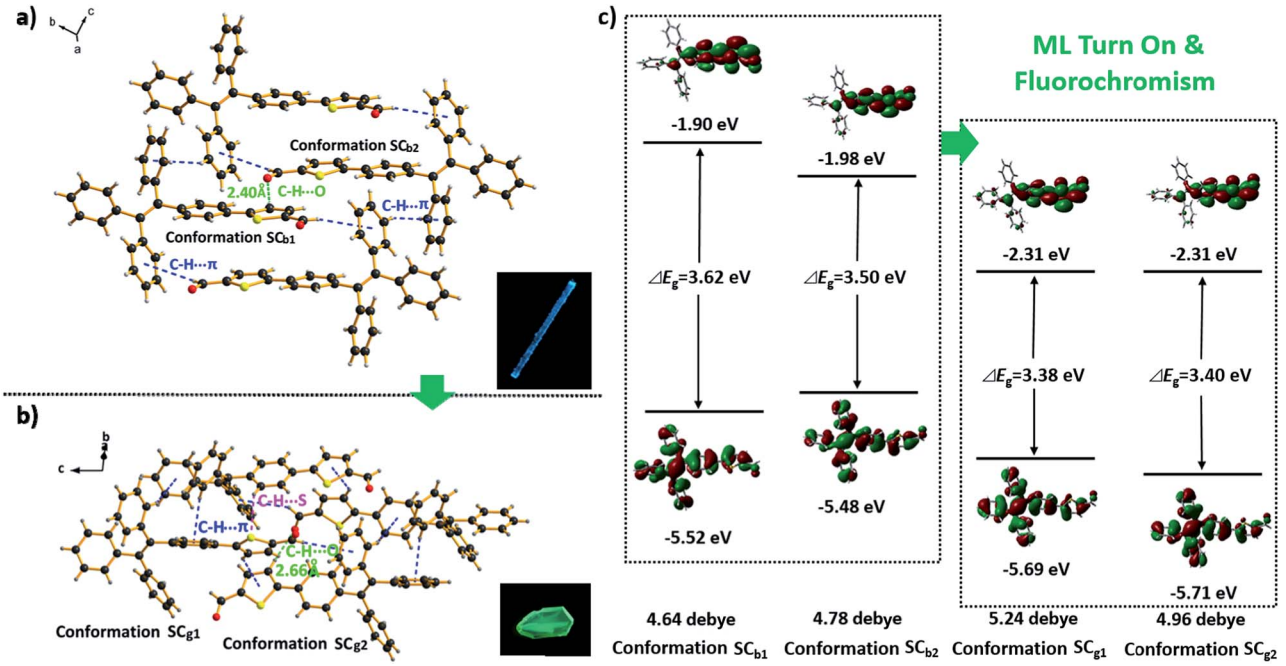

Fig. 5 Stacking modes and intermolecular interactions of the molecules in polymorphs SC_b (a) and SC_g (b); the insets show the fluorescence images of SC_b and SC_g under an excitation of 365 nm UV light. (c) The HOMO (lower images) and LUMO (upper images) of the four conformations of P_4TA in polymorphs SC_b and SC_g calculated at the B3LYP/6-31G(d, p) level.

the requirements for piezoelectric properties, thus making the as-prepared crystals of C_g and C_b more active and more likely to achieve the ML character. However, the dipole moments and the HOMO–LUMO band gaps (ΔE_g) of the molecules in the SC_g and SC_b polymorphs were different. These differences were caused by their distinct molecular conformations and packing characteristics. The asymmetric units in both polymorphs (*i.e.*, SC_g and SC_b) were composed of two crystallographically independent molecules (*i.e.*, SC_{g1} and SC_{g2} for SC_g, and SC_{b1} and SC_{b2} for SC_b). Each molecule showed the formation of a C–H···O intermolecular hydrogen bond (Fig. 5a and b, S3 and S4†). Compared with SC_b, the most notable conformational difference of P_4TA in the SC_g polymorph was the dihedral angle θ between the thiophene and the adjacent phenyl ring. While the conformations of P_4TA were twisted ($\theta = 18.9°$ for SC_{g1} and 6.1° for SC_{g2}) in polymorph SC_g, the two aromatic rings were nearly coplanar in polymorph SC_b ($\theta = 2.5°$ for SC_{b1} and 4.7° for SC_{b2}) (Table S2†). In the case of SC_g, the two thiophene rings of SC_{g1} and SC_{g2} were almost perpendicular to each other, showing a dihedral angel of 85.8°. By contrast, an anti-parallel packing mode was observed between the thiophene rings of SC_{b1} and SC_{b2} ($\theta = 3.7°$) in SC_b.

The most popular B3LYP density functional theory was then used to calculate the dipole moments and the ΔE_g of P_4TA in the four conformations at the 6-31G(d, p) level based on their ground state geometries in the single crystals. Fig. 5c presents the results. The dipole moments of SC_{g1} and SC_{g2} in the SC_g polymorph were 5.24 and 4.96 debye (D), respectively. Both values were larger than those of SC_{b1} (4.64 D) and SC_{b2} (4.78 D) in SC_b. The larger dipole moments of the molecules combining the non-centrosymmetric molecular arrangement may result in a larger net-dipole moment of the crystalline structure, and would subsequently lead to a stronger piezoelectric effect in the SC_g polymorph when breaking the crystals. The theoretical calculation results also suggest that the molecules in both SC_g and SC_b have ICT characteristics: the electronic transitions (mainly from HOMO to LUMO for all the four conformations in SC_g and SC_b) from the occupied orbitals delocalized over the TPE (donor) moiety to the thiophenaldehyde (acceptor) moiety made major contributions to the excited states (Fig. 5c and Table S4†).[16] SC_{g1} and SC_{g2} showed even smaller ΔE_g (HOMO → LUMO) values of 3.38 and 3.40 eV, respectively, as compared to those of SC_{b1} (3.62 eV) and SC_{b2} (3.50 eV) in the SC_b polymorph. The calculations showed good agreement with the solid state UV-visible spectra of C_g and C_b, which absorbed at 373 nm and 367 nm, respectively (Fig. S5†). The preceding results thus indicate that the electrons of the molecules in SC_g can be excited with a lower energy. Hence, the stronger piezoelectric effect and the lower electronic transition energy resulted in the excitation of P_4TA molecules and the generation of ML in the SC_g phase by breaking the crystals. Meanwhile, all the molecules adopted a highly twisted propeller-like conformation in the SC_g polymorph, which prevented the formation of detrimental species, such as excimers or exciplexes, caused by π–π stacking interactions. Furthermore, numerous intermolecular interactions such as C–H···π and C–H···S might also exist in the crystals aside from the C–H···O hydrogen bonding (Fig. 5b and Table S3†). These multiple interactions had rigidified the molecular conformations and impeded intramolecular rotation, which largely reduced the energy loss *via* non-radiative

relaxation channels, and subsequently resulted in a notable AIE effect and high $\Phi_{F,s}$ value for P_4TA. The preceding factors consequently made the ML of sample C_g, which was mainly composed of P_4TA microcrystals in the SC_g polymorph, highly emissive under the stimulus of mechanical force. By contrast, the weaker piezoelectric effect in the SC_b polymorph seemed not to reach the higher energy requirement for the electronic excitation although SC_b also exhibited strong photoluminescence. Consequently, P_4TA lost its ML activity when aggregated in the C_b phase. These results also suggest a feasible design direction for the development of efficient ML materials through combining the prominent piezoelectric property for molecular excitation and the abnormal AIE character for emission.

The PL of C_b was remarkably changed when the sample was exposed to DCM or acetone vapors for about 10 min, passing from an initial blue to green light at 499 nm (C_{bf}-form). The resulting spectrum of C_{bf} was superimposable on that of C_g (Fig. 2b). The coincidence of the PL emissions suggested that the fumed sample of C_{bf} probably had the same molecular arrangement as that of the C_g polymorph. Further evidence for this standpoint was provided by their similar XRD patterns and their overlapping DSC curves with the same melting point at 206 °C (Fig. 4a and b). As mentioned in the preceding discussion, sample C_g was ML-active. And expectantly, the ML activity of C_b could be tuned by simply altering the molecular packing mode upon fumigation. To verify this hypothesis, the ML spectrum of C_b was collected after exposure to DCM vapor (C_{bf}). As anticipated, C_{bf} also exhibited a strong green light emission without UV irradiation using pressure, which revealed that the ML of C_b could be facilely turned on with the aid of DCM vapor. The ML emission maximum of C_{bf} was located at 520 nm, which is close to that of C_g (Fig. 3a).

Noticeably, the ML maxima of C_g and C_{bf} were both significantly red-shifted ($\Delta\lambda_{em,max} \approx 21$ nm) as compared to their PL spectra. This result shows a special mechanofluorochromic effect. To gain an understanding of this, the influence of applied pressure on the luminescence was investigated. The PL maximum of the pristine P_4TA in the C_g-form shifted from 498 nm to 521 nm (G_g) after pressing or grinding (Fig. 2a), agreeing well with its ML emission (Fig. S6†), thereby confirming that the bathochromic shift between the ML and PL of C_g was caused by its intrinsic mechanochromic properties. The phase characteristics of the ground sample G_g were determined by XRD to decipher further the relationship between the ML and the mechanochromism of C_g. Most of the diffraction peaks were diffuse or even disappeared, although some resolvable peaks of G_g were consistent with those of their original crystals (Fig. 6a). This revealed that the ground sample was partially in a metastable amorphous state. Accordingly, DSC was performed for the sample after grinding (Fig. 6b). Compared with C_g, an additional exothermal peak around 86 °C was observed in the DSC thermogram of G_g, which demonstrated that the C_g crystals were partially destroyed and converted to an amorphous state by the grinding or pressing treatment. The P_4TA molecules in the C_g phase adopt twisted conformations in the crystalline state to

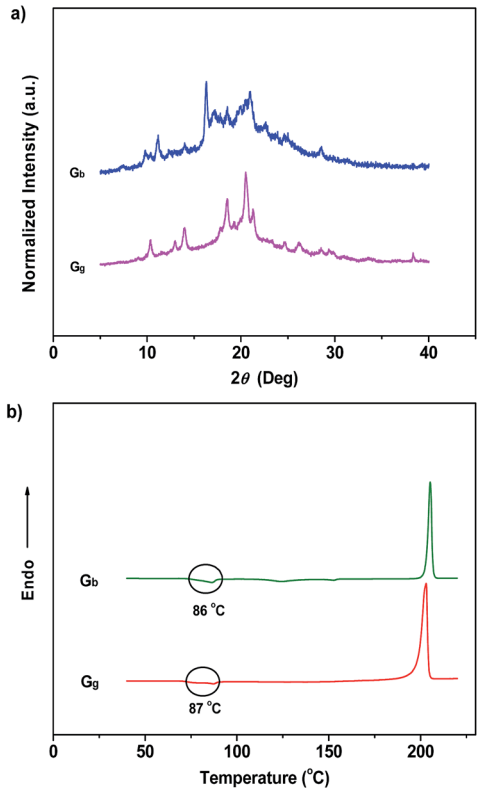

Fig. 6 XRD patterns (a) and DSC curves (b) of the ground samples of P_4TA: (G_b) ground sample from the blue-light crystals; (G_g) ground sample from the green-light crystals.

fit into the crystalline lattice, and the crystalline lattices may collapse when triggered with mechanical force. The dye molecules also then relaxed to a more planar conformation, thereby emitting redder ML and PL. In other words, the bathochromic shift of the ML for C_g originates from the microcrystal amorphization and the extension of molecular conjugation, which were believed to be the main reasons for the C_g mechanochromism.[16,17] Unlike other conventional stimuli-responsive materials, the C_g-form of P_4TA can show a luminescence response and luminescence color change simultaneously and respectively both without and with UV irradiation under a force stimulus. This new kind of force-responsive material with AIE properties has not yet been achieved before, and would facilitate applications of ML materials in the field of sensors.[11c] In addition, fluorescence spectroscopy was also performed to evaluate the mechanochromic behavior of P_4TA in the C_b phase, and the C_b sample exhibited a more remarkable emission wavelength change of 47 nm upon grinding. Furthermore, the corresponding PL spectrum (G_b) with $\lambda_{em,max} = 523$ nm fitted well with that for the powder ground from C_g (Fig. 2b), which indicated that P_4TA could switch to the same emission under a force stimulus regardless of its initial state. Also the fluorescence 'writability' of C_b can be verified by writing on a piece of filter paper as shown in Fig. 3d. The mechanofluorochromism of C_b should occur by a similar mechanism to that proposed for C_g.

Conclusions

Based on AIE-active P_4TA molecules, two photoluminescent polymorphs (*i.e.*, C_g and C_b) with multiple molecular conformations were achieved. They can show opposing mechanoluminescence activities by tuning the molecular assembly structures in the crystals. The block-like crystals of C_g exhibited a very bright green color ML upon pressing or grinding under daylight at room temperature. This unique property should be attributed to the strong piezoelectric effect of the crystals and the positive effect of the AIE property on luminescence enhancement. Moreover, with UV irradiation, the C_g of P_4TA showed mechanofluorochromism under a mechanical stimulus. This new kind of force-responsive compound with an AIE property could facilitate the application of ML materials in the display and sensor fields. This work may provide a feasible design direction for the development of more efficient ML materials by combining the prominent piezoelectric property for molecular excitation and the unique AIE character for emission.

Acknowledgements

The authors gratefully acknowledge financial support from the NSF of China (51173210, 51073177), the Fundamental Research Funds for the Central Universities and NSF of Guangdong (S2011020001190).

Notes and references

1 (*a*) N. C. Eddingsaas and K. S. Suslick, *Nature*, 2006, **444**, 163; (*b*) N. C. Eddingsaas and K. S. Suslick, *J. Am. Chem. Soc.*, 2007, **129**, 6718.

2 S. M. Jeong, S. Song, K. I. Joo, J. Kim, S. H. Hwang, J. Jeong and H. Kim, *Energy Environ. Sci.*, 2014, **7**, 3338.

3 (*a*) S. Moon Jeong, S. Song, S. K. Lee and B. Choi, *Appl. Phys. Lett.*, 2013, **102**, 051110; (*b*) S. M. Jeong, S. Song, S. K. Lee and N. Y. Ha, *Adv. Mater.*, 2013, **25**, 6194; (*c*) D. O. Olawale, T. Dickens, W. G. Sullivan, O. I. Okoli, J. O. Sobanjo and B. Wang, *J. Lumin.*, 2011, **131**, 1407; (*d*) I. Sage and G. Bourhill, *J. Mater. Chem.*, 2001, **11**, 231; (*e*) Y. Tsuboi, T. Seto and N. Kitamura, *J. Phys. Chem. B*, 2003, **107**, 7547.

4 (*a*) G. E. Hardy, J. C. Baldwin, J. I. Zink, W. C. Kaska, P. H. Liu and L. Duboisi, *J. Am. Chem. Soc.*, 1997, **99**, 3552; (*b*) L. M. Sweeting, A. L. Rheingold, J. M. Gingerich, A. W. Rutter, R. A. Spence, C. D. Cox and T. J. Kim, *Chem. Mater.*, 1997, **9**, 1103; (*c*) L. M. Sweeting, *Chem. Mater.*, 2001, **13**, 854.

5 H. Nakayama, J. I. Nishida, N. Takada, H. Sato and Y. Yamashita, *Chem. Mater.*, 2012, **24**, 671.

6 (*a*) G. E. Hardy, J. I. Zink, W. C. Kaska and J. C. Baldwin, *J. Am. Chem. Soc.*, 1978, **100**, 8001; (*b*) G. E. Hardy, W. C. Kaska, B. P. Cbandra and J. I. Zink, *J. Am. Chem. Soc.*, 1981, **103**, 1074; (*c*) E. Boldyreva, *Chem. Soc. Rev.*, 2013, **42**, 7719.

7 (*a*) H. Y. Zhang, Z. L. Zhang, K. Q. Ye, J. Y. Zhang and Y. Wang, *Adv. Mater.*, 2006, **18**, 2369; (*b*) K. Wang, H. Zhang, S. Chen, G. Yang, J. Zhang, W. Tian, Z. Su and Y. Wang, *Adv. Mater.*, 2014, **26**, 6168.

8 L. M. Sweeting and A. L. Rheingoldf, *J. Am. Chem. Soc.*, 1987, **109**, 2652.

9 (*a*) R. Jakubiak, C. J. Collison, W. C. Wan, L. J. Rothberg and B. R. Hsieh, *J. Phys. Chem. A*, 1999, **103**, 2394; (*b*) K. C. Wu, P. J. Ku, C. S. Lin, H. T. Shih, F. I. Wu, M. J. Huang, J. J. Lin, I. C. Chen and C. H. Cheng, *Adv. Funct. Mater.*, 2008, **18**, 67; (*c*) P. Galer, R. C. Korošec, M. Vidmar and B. Šket, *J. Am. Chem. Soc.*, 2014, **136**, 7383.

10 (*a*) J. Luo, Z. Xie, J. W. Y. Lam, L. Cheng, B. Z. Tang, H. Chen, C. Qiu, H. S. Kwok, X. Zhan, Y. Liu and D. Zhu, *Chem.Commun.*, 2001, 1740; (*b*) B. K. An, S. K. Kwon, S. D. Jung and S. Y. Park, *J. Am. Chem. Soc.*, 2002, **124**, 14410; (*c*) H. Tong, Y. Hong, Y. Dong, M. Häußler, J. W. Y. Lam, Z. Li, Z. Guo, Z. Guo and B. Z. Tang, *Chem. Commun.*, 2006, 3705; (*d*) W. Z. Yuan, P. Lu, S. Chen, J. W. Y. Lam, Z. Wang, Y. Liu, H. S. Kwok, Y. Ma and B. Z. Tang, *Adv. Mater.*, 2010, **22**, 2159; (*e*) B. Xu, M. Xie, J. He, B. Xu, Z. Chi, W. Tian, L. Jiang, F. Zhao, S. Liu, Y. Zhang, Z. Xu and J. Xu, *Chem. Commun.*, 2012, **49**, 273; (*f*) C. Li, T. Wu, C. Hong, G. Zhang and S. Liu, *Angew. Chem., Int. Ed.*, 2011, **51**, 455.

11 (*a*) Y. Hong, J. W. Y. Lam and B. Z. Tang, *Chem. Commun.*, 2009, 4332; (*b*) Y. Hong, J. W. Y. Lam and B. Z. Tang, *Chem. Soc. Rev.*, 2011, **40**, 5361; (*c*) Z. Chi, X. Zhang, B. Xu, X. Zhou, C. Ma, Y. Zhang, S. Liu and J. Xu, *Chem. Soc. Rev.*, 2012, **41**, 3878; (*d*) Z. Zhao, J. W. Y. Lam and B. Z. Tang, *J. Mater. Chem.*, 2012, **22**, 23726; (*e*) Y. Gong, Y. Zhang, W. Z. Yuan, J. Z. Sun and Y. Zhang, *J. Phys. Chem. C*, 2014, **118**, 10998.

12 (*a*) B. Xu, Z. Chi, H. Li, X. Zhang, X. Li, S. Liu, Y. Zhang and J. Xu, *J. Phys. Chem. C*, 2011, **115**, 17574; (*b*) Z. Yang, W. Qin, J. W. Y. Lam, S. Chen, H. H. Y. Sung, I. D. Williams and B. Z. Tang, *Chem. Sci.*, 2013, **4**, 3725.

13 (*a*) J. I. Zink and W. Klimt, *J. Am. Chem. Soc.*, 1974, **96**, 4960; (*b*) P. Jha and B. P. Chandra, *Luminescence*, 2014, **29**, 977.

14 (*a*) S. Biju, N. Gopakumar, J. C. G. Bünzli, R. Scopelliti, H. K. Kim and M. L. P. Reddy, *Inorg. Chem.*, 2013, **52**, 8750; (*b*) S. Balsamy, P. Natarajan, R. Vedalakshmi and S. Muralidharan, *Inorg. Chem.*, 2014, **53**, 6054.

15 L. S. McCarty and G. M. Whitesides, *Angew. Chem., Int. Ed.*, 2008, **47**, 2188.

16 R. Misra, T. Jadhav, B. Dhokale and S. M. Mobin, *Chem. Commun.*, 2014, **50**, 9076.

17 (*a*) W. Z. Yuan, Y. Tan, Y. Gong, P. Lu, J. W. Y. Lam, X. Y. Shen, C. Feng, H. H. Y. Sung, Y. Lu, I. D. Williams, J. Z. Sun, Y. Zhang and B. Z. Tang, *Adv. Mater.*, 2013, **25**, 2837; (*b*) Y. Gong, Y. Tan, J. Liu, P. Lu, C. Feng, W. Z. Yuan, Y. Lu, J. Z. Sun, G. He and Y. Zhang, *Chem. Commun.*, 2013, **49**, 4009; (*c*) P. Gautam, R. Maragani, S. M. Mobin and R. Misra, *RSC Adv.*, 2014, **4**, 52526.